Loughborough University

This item was submitted to Loughborough's Research Repository by the author.
Items in Figshare are protected by copyright, with all rights reserved, unless otherwise indicated.

Spectral response measurements of Perovskite solar cells

PLEASE CITE THE PUBLISHED VERSION

https://doi.org/10.1109/JPHOTOV.2018.2878003

PUBLISHER

Institute of Electrical and Electronics Engineers

VERSION

VoR (Version of Record)

PUBLISHER STATEMENT

This work is made available according to the conditions of the Creative Commons Attribution 3.0 Unported (CC BY 3.0) licence. Full details of this licence are available at: http://creativecommons.org/licenses/by/3.0/

LICENCE

CC BY 3.0

REPOSITORY RECORD

Bliss, Martin, Alex Smith, Tom Betts, Jenny Baker, Francesca De Rossi, Sai Bai, Trystan Watson, Henry Snaith, and Ralph Gottschalg. 2019. “Spectral Response Measurements of Perovskite Solar Cells”. figshare. https://hdl.handle.net/2134/35595.

Spectral Response Measurements of Perovskite Solar Cells

Martin Bliss, Alex Smith, Thomas R. Betts, Jenny Baker, Francesca De Rossi, Sai Bai, Trystan Watson, Henry Snaith, and Ralph Gottschalg

***Abstract*—A new spectral response (SR) measurement routine is proposed that is universally applicable for all perovskite devices. It is aimed at improving measurement accuracy and repeatability of SR curves and current–voltage curve spectral mismatch factor (MMF) corrections. Frequency response, effects of preconditioning as well as dependency on incident light intensity and voltage load on SR measurements are characterized on two differently structured perovskite device types. It is shown that device preconditioning affects the SR shape, causing errors in spectral MMF corrections of up to 0.8% when using a reference cell with a good spectral match and a class A solar simulator. Wavelength dependent response to incident light intensity and voltage load is observed on both device types, which highlights the need to measure at short-circuit current and maximum power point to correct spectral mismatch. The method with recommendations given ensures that the correct measurement conditions are applied and measurements are corrected for instability in performance.**

***Index Terms*—Characterization, perovskite, quantum efficiency, spectral response (SR).**

Manuscript received June 26, 2018; accepted October 15, 2018. Date of publication November 14, 2018; date of current version December 21, 2018. This work was supported by the EPSRC SUPERGEN SuperSolar Hub (EP/J017361/1) and also by the EMPIR Programme co-financed by the Participating States and from the European Union's Horizon 2020 research and innovation programme. The work of M. Bliss was supported by the British Council Newton Fund Institutional Link Project: Enhancement of Photovoltaic and Wind Turbine Performance for High Temperature and Low Wind Speed Environments. *(Corresponding author: Martin Bliss.)*

M. Bliss, A. Smith, and T. R. Betts are with the Centre for Renewable Energy Systems Technology, Wolfson School Mechanical, Electronic and Manufacturing Engineering, Loughborough University, Loughborough LE11 3TU, U.K. (e-mail: M.Bliss@lboro.ac.uk; A.Smith8@lboro.ac.uk; T.R.Betts@lboro.ac.uk).

J. Baker, F. De Rossi, and T. Watson are with SPECIFIC, Swansea University, Swansea SA1 8EN, U.K. (e-mail: j.baker@swansea.ac.uk; f.derossi@swansea.ac.uk; T.M.Watson@swansea.ac.uk).

S. Bai was with the Department of Physics, University of Oxford, Oxford OX1 3PU, U.K. He is now with Department of Physics, Chemistry and Biology (IFM), Linköping University, Linköping SE-58183 Sweden (e-mail: sai.bai@liu.se).

H. Snaith is with the Department of Physics, Clarendon Laboratory, University of Oxford, Oxford OX1 3PU, U.K. (e-mail: Henry.Snaith@physics.ox.ac.uk).

R. Gottschalg was with the Centre for Renewable Energy Systems Technology, Loughborough University, Loughborough LE11 3TU, U.K. He is now with Fraunhofer-Center for Silicon-Photovoltaic, 06120 Halle, Germany, and also with the Fachbereich Elektrotechnik, Maschinenbau und Wirtschaftsingenieurwesen (EMW), Hochschule Anhalt, 06366 Köthen, Germany (e-mail: Ralph.Gottschalg@csp.fraunhofer.de).

Color versions of one or more of the figures in this paper are available online at http://ieeexplore.ieee.org.

Digital Object Identifier 10.1109/JPHOTOV.2018.2878003

I. Introduction

PEROVSKITE solar cells have gained significant interest and importance over the past years with independently verified efficiencies now surpassing 20.9% on $\sim$1 cm^2 solar cells [1], [2] and 16% on minimodules [1]. Independent verification of device efficiency is important when comparing device performance between research labs. This is particularly challenging for perovskite solar cells as their general behavior under measurement is different to more conventional photovoltaic devices. The key problem arising with perovskite solar cells is the metastability causing a change in performance dependent on the operational history. Measurements are affected by a hysteresis when measuring the current–voltage (*I–V*) curve in forwards and reverse directions, which is somewhat similar to high capacitance silicon or dye-sensitized solar cells. However, the origin of this hysteresis effect is different. The device is affected by metastability with respect to voltage and irradiance history in the time-scale of typical measurements [3]–[7], also referred to as preconditioning effects. This makes the use of common measurement routines using flash solar simulators impossible and increases the difficulty in characterizing these devices as conventional measurement approaches deliver inaccurate results. This is demonstrated by an inter-laboratory comparison, which reported much larger variability in efficiency measurements of perovskite samples compared to silicon solar cells [8]. Unaccredited research labs in the inter-comparison showed a $\sim$35% standard deviation in reported efficiency of slow responding perovskite devices compared to $\sim$3.7% of silicon solar cells. The comparability between laboratories was much better on fast responding devices, but nevertheless still 30% higher compared to silicon samples.

The magnitude of the effects described can change between different device structures or even from batch to batch of the same technology. Device inter-comparisons and quality assessments require a standardized methodology considering all idiosyncrasies. This is important for both *I–V* curve and spectral response (SR) or external quantum efficiency (EQE) measurements. While methodologies for *I–V* measurements of perovskite devices have been investigated [8]–[11], much less is reported on the applicability of SR measurement methods [9]. Nevertheless, SR measurements are a significant step in the calibration of devices. They are required to calculate the spectral mismatch factor (MMF) [12] that corrects the device performance measurements from the error induced by the

This work is licensed under a Creative Commons Attribution 3.0 License. For more information, see http://creativecommons.org/licenses/by/3.0/

differences between the solar simulator spectrum and the standardized test spectrum [13]. This step is often not carried out and the somewhat questionable approach of using a "matched" reference cell (RC) is chosen. This paper investigates the difficulties associated with determination of the SR.

The focus of this work is on how different SR measurement parameters, such as bias irradiance, voltage load, preconditioning, and modulation frequency affect results. The objective is not to explain physical causes of effects, but rather to develop a universally applicable methodology to measure the SR with good reliability and repeatability. Guidelines are provided that will enable better inter-laboratory comparability for accredited measurement laboratories and material research laboratories. While test device temperature also affects SR with wavelength dependency to varying degrees, this has not been investigated here due to difficulties contacting the superstrate test devices. Temperature coefficients of perovskite solar cells are reviewed in [14] and the impact on SR has been investigated in [15].

To highlight the variability in performance characteristic and behavior of differently structured devices, the characteristics of two different perovskite architectures are investigated: Sample type A, $\sim$10 mm^2 small area round samples with a p-i-n planar heterojunction structure similar to [16] but with NiO and PCBM as the p-type and n-type charge extraction layer. The perovskite active layer of type A is a triple cation perovskite with the same composition as in [17] and sample type B, 1 cm^2 area perovskite device with a triple mesoscopic structure, i.e., overlapped mesoporous titania, zirconia, and carbon, as detailed in [18] using two-dimensional/three-dimensional $(HOOC(CH_2)4NH_3)_2PbI_4/CH_3NH_3PbI_3$ perovskite for better stability [19]. For comparison purposes, the efficiency and fill factor of device type A was measured as $\eta = 12.5\%$, FF $= 75\%$ and of type B as $\eta = 6.7\%$, FF $= 33\%$.

Better SR measurements lower the uncertainty in MMF corrections as will be shown in the following. MMF error estimates are given to provide a guide to the impact of imperfect SR measurements. They are based on a typical class A spectral match [20] solar simulator using a moderately well-matched KG2 filtered RC. The error induced will vary from system to system and can be significantly higher as it is heavily dependent on the solar simulator spectrum and RC used.

II. Measurement Facilities

A multi-laser high-speed EQE system has been utilized for this work. The system can measure a full 11-point EQE curve in as little as 0.1 s, synchronized for all wavelengths at the same time. The system is therefore capable of recording the dynamic changes in perovskite solar cell performance due to preconditioning and variations in electrical load or in irradiance incident on the cell. This provides additional understanding of the behavior of perovskite solar cells that cannot be provided using conventional systems that scan the SR curve with each wavelength consecutively.

The principle of the system is based on a method utilized in [21]: The laser light is sine-wave modulated with adjustable frequency and intensity. The current signals from the reference diode and sample are extracted using fast Fourier transformation. Because all lasers can be modulated at the same time at different frequencies, the full 11-point differential spectral response curve can be extracted for all wavelengths simultaneously. The system projects an over-illuminating monochromatic light beam onto the device under test (DUT). In total, 11 diode lasers at varying wavelengths 405 to 1060 nm are used as monochromatic light sources. By default, a 160 to 340 Hz range with a 10 Hz separation and rejecting 50 Hz power line harmonics is used. As will be shown in Section III-B, measuring all wavelengths simultaneously at ac had little influence on the shape of SR curve of both device types tested. The typical irradiance for all lasers illuminating the sample simultaneously is $\sim$0.5 mW/cm^2. The bias light consists of 4000 K natural white LED lamps that can reach an equivalent effective light intensity of $\sim$1.5 suns on a silicon solar cell. Because the test samples are both superstrate configuration, temperature control of the devices during measurements was not possible. Nevertheless, because white LED bias light is used without infrared (IR) component, the effect on temperature during measurements is reduced even at 1 Sun equivalent light intensity.

The laser SR system is comparison calibrated using a silicon RC traceable to the European Solar Test Installation.

III. Device Behavior and Measurement Implications

A. Preconditioning

It is well known that preconditioning of perovskite samples is one cause of hysteresis during *I–V* curve measurements. Thus, preconditioning effects have been measured to quantify the dependence on SR. In addition to periodically measured DUT bias voltage, current, and irradiance, the EQE curve is measured as a "snapshot" simultaneously using all lasers as detailed in the previous section. The preconditioning profile was 20 min of light soaking with 10 min of relaxation before and after light soaking. Bias voltage was applied from the start and throughout the full test. Light soaking was recoded at multiple bias light and voltage conditions; however, for relevance, only results from preconditioning at I_{SC} are shown here.

Significant differences are observed in the current traces of both sample types measured during preconditioning (top graph of Fig. 1). Type A responds much faster and type B settles more slowly. However, both devices needed $\sim$10–15 min to stabilize. The rate of this is dependent on bias irradiance, with faster stabilization at lower irradiance and smaller voltage bias, with longer settling for higher voltage load. Also noted was a slow gradual increase in current readings even after 20 min of light soaking on type A devices, which can affect especially SR measurements that are taken very slowly. During preconditioning, both device types showed significant changes in the absolute scale of the EQE curve, as indicated by the current measurements, and also in the relative EQE curve shape. The bottom graph of Fig. 1 compares the relative EQE measured at the beginning of light soaking just after turning on the 1 Sun intensity bias light to the end just before switching off the bias light. A change in EQE shape is observed on both samples, but with opposite trend. Type B shows a significant increase in red to near IR (NIR)

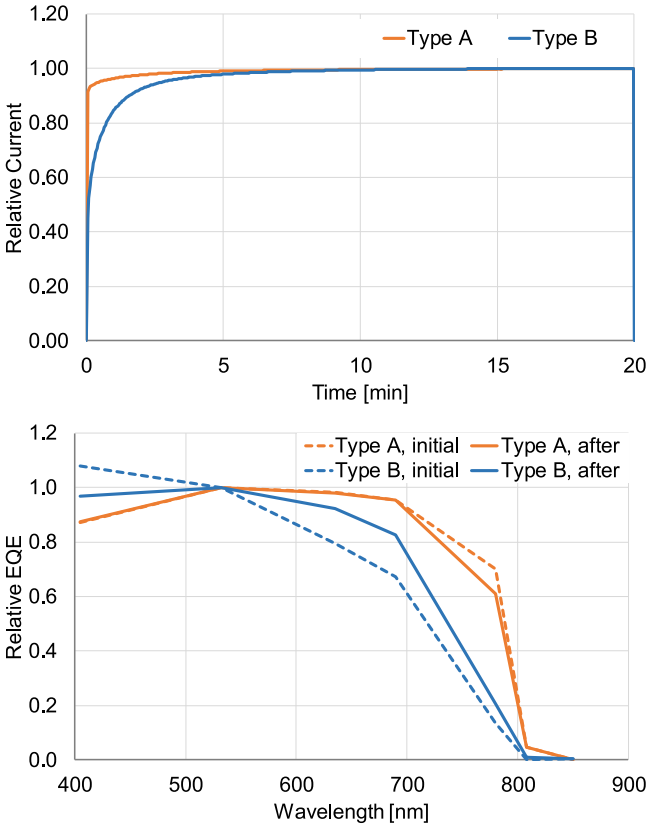


Fig. 1. Top: Measured current during light soaking at 1 Sun at I_{SC} (0 voltage bias). Bottom: Change in relative EQE due to light soaking from initial measurement to after 20 min light soaking; a change in relative EQE is observed in both devices with different trends.

response and a reduction in blue light absorption, whereas on device type A, a reduction in relative EQE in the NIR region is observed. While a detailed investigation as to the exact cause has not been investigated in this work, it is estimated that the main cause in the difference in response can be attributed to the different perovskite materials and likely device structures between device type A and B. The effect on MMF between initial EQE and EQE after 20 min of light soaking is in this case small for type A with 0.03% and significant for type B with 0.8% change in MMF. Note that some of the changes in the shape of the SR may be caused by changing sample temperature during preconditioning.

The results detailed in Fig. 1 highlight the importance of allowing for stabilization of the DUT under bias light and voltage load conditions before starting measurements. Preconditioning affects not only the absolute scale of the EQE, but also the shape, which influences MMF and thus *I–V* curve and efficiency measurements. Because EQE is normally scanned at consecutive wavelengths or filters one by one, not allowing for preconditioning can cause an additional error due to changing performance of the DUT during the measurement as shown in Fig. 2. Here, the EQE is measured in this example consecutively over the first 6 min after enabling the bias light. In this case, the shape of the EQE curve especially of type B is significantly skewed. The MMF is affected by absolute 0.1% on type A and 0.55% on type B.

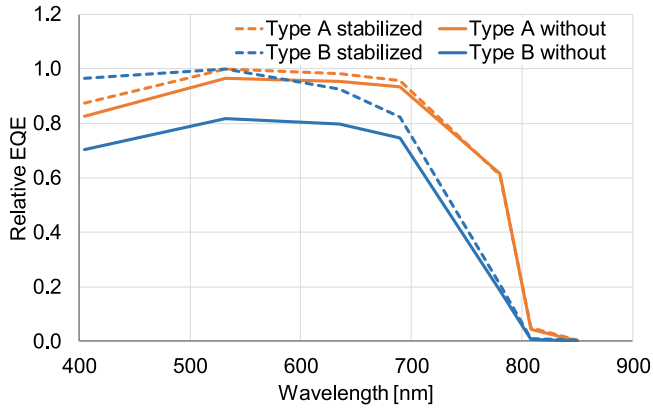


Fig. 2. Measurement error caused during scanning of the EQE curve without allowing the device to stabilize to its bias conditions.

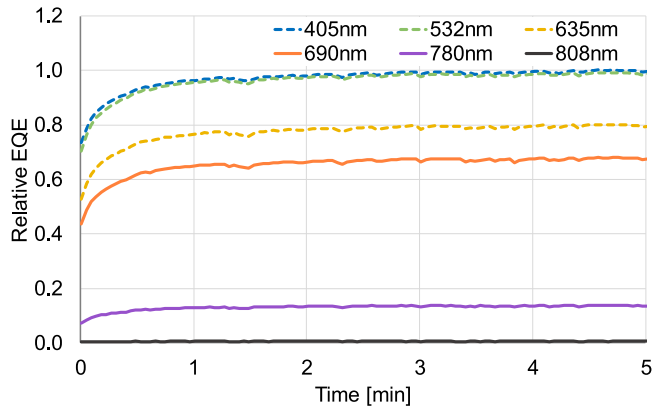


Fig. 3. Preconditioning influenced by monochromatic light of Laser EQE system at 0 V load without bias light. Results of device type B shown here, type A shows a faster stabilization.

Because type A devices have shown a very slow improvement even after 20 min of preconditioning, it is important to monitor the sample current during SR measurements. For complete confidence that device performance has not changed significantly and affected SR measurements, it is advisable to monitor a reference wavelength at least before and after the SR measurements. The bias current of the DUT should be monitored throughout the measurement. The recorded data can then be used to correct the SR curve for instability in performance, as detailed in Section IV.

To save time, one could consider measuring in the dark without bias light. However, it was observed that the measured EQE increased significantly over the first minute with little wavelength dependence (see Fig. 3). This was caused by preconditioning of the perovskite devices due to the monochromic laser light used for measurements. Both sample types show a similar response to varying rate. At 0.2 Suns bias light intensity, this effect was not evident because the intensity of the monochromatic light was much smaller than the bias light. For accurate SR measurements, this means samples should not be measured without bias light. Even though the change in SR is independent of wavelength at low light preconditioning, the change in its scale is significant. When the SR curve is traced with monochromatic

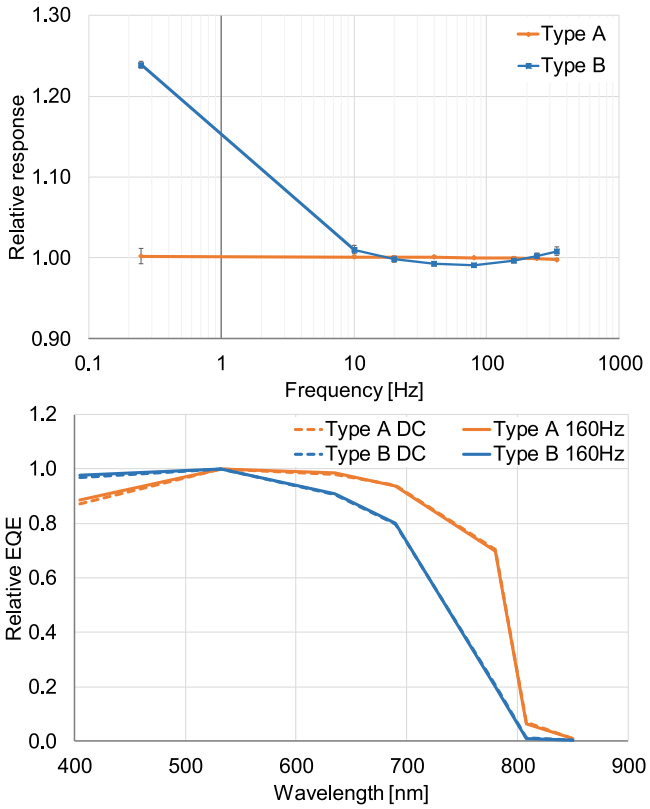


Fig. 4. Top: Frequency response of EQE measurements from dc (∼0.25 Hz) to 340 Hz; error bars indicate standard deviation of response between wavelengths; Bottom: Relative EQE curve shape at dc and at 160 Hz; the impact on MMF measuring at 160 Hz instead of dc is considered below overall measurement uncertainty even though the absolute scale is affected on type B devices.

light only, the device will precondition to varying degrees depending on the intensity of the monochromatic light beam and the response to it. This results in a relative error in the SR curve that affects MMF in a way similar to that shown in Fig. 2. More importantly though, as will be shown in the following sections, the SR of both devices tested showed wavelength dependent nonlinearity to bias light intensity, meaning an MMF error is introduced by measuring in the dark to begin with.

B. Frequency Response

The majority of SR measurement systems uses chopped light and lock-in amplification to extract the SR signal from the bias and noise. Previously, the modulation frequency was shown to have a significant impact on SR measurements of dye-sensitized solar cells [22]–[24], which are also known for significant *I–V* curve measurement hysteresis [25], [26]. Thus, it is important to investigate the possible measurement artifacts on perovskite devices, given the common features. The wavelength averaged frequency response of EQE measurements of both perovskite device types is detailed in the top graph of Fig. 4. The samples were illuminated at ∼200 W/m^2 and preconditioned for a minimum of 10 min before testing. Error bars indicate the standard deviation in frequency response between the laser signals. A low standard deviation therefore means that the EQE response maintains a consistent shape.

Both device types show a good flat response within the range of 10–340 Hz. The near-dc response (4 s per measurement, ∼0.25 Hz) of type B is significantly larger than at 10 Hz. However, as shown in bottom graph of Fig. 4, the change in frequency response affects mainly the absolute scale of the EQE while the shape changes only by a small extent. The increased dc response was noted on both type B samples available for testing with some variation in the increase in response relative to ac (24% and 20%). This is unlikely to arise in the measurement system and it cannot be attributed to electrical low-pass filtering such as the capacitive response of the sample because of the flat response seen at higher frequencies. The effect on MMF between measuring at dc and at 160 Hz is 0.05% for type A and 0.04% for type B, using a class A Xenon lamp solar simulator with a KG2 filtered silicon RC.

Because both types show differing frequency response, as shown in Fig. 4, the effect of modulation frequency on EQE should be verified before measuring. Type B showed a significant increase in SR amplitude at dc, which suggests that one should always measure under dc because it is more representative of real outdoor conditions. However, this may not be beneficial for measurement accuracy. Measurements at dc are much more prone to low frequency bias light fluctuations and noise from amplifiers, which take a long time to average out. Measuring in the dark improves the measurement signal, however, as shown in the previous section, it introduces a significant error in both the EQE scale and shape, affecting also the MMF correction for *I–V* curve measurements. Therefore, if the DUT shows a flat response area at higher frequencies that has little or no effect on the shape of the EQE curve, as shown in this case for both device types, the conclusion is that it is better overall to measure with chopped light. The lock-in amplifier technique can then be utilized to reduce noise influence and eliminate low frequency bias light errors caused by power supply and temperature variations. The absolute scale error in the SR curve can be corrected using I_{SC} measurements under broadband illumination and is irrelevant for MMF corrections. The estimated MMF error introduced in the presented case (0.05%) by measuring using modulated light is considered well below uncertainties introduced by measuring under dc.

C. Influence of Bias Light and Voltage on Steady-State Conditions

The accuracy of MMF corrections to *I–V* measurements, especially of wavelength-dependent nonlinear devices, depends heavily on the applied bias irradiance conditions [27], [28]. In addition to irradiance bias, the voltage load on the DUT also can influence the sample SR, as reported for amorphous silicon devices [29], [30]. This section investigates the effect of bias light intensity and voltage load on SR measurements and its impact on MMF. The bias light influence was measured at I_{SC} (0 V) and the voltage bias dependency was measured at 1 Sun intensity. After 10 min preconditioning, at which time the devices are at, or near, static conditions, the current, voltage, and EQE were recorded.

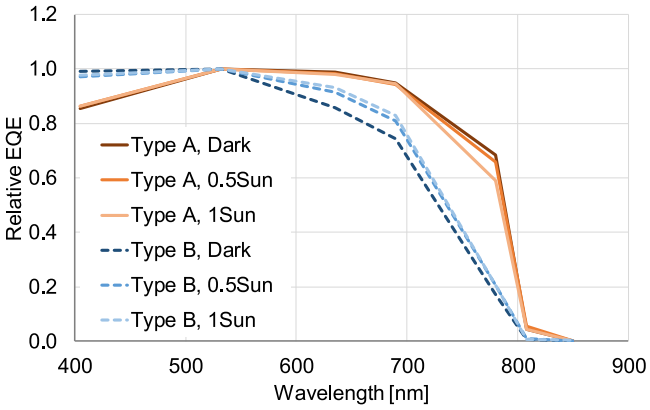


Fig. 5. Relative EQE at different bias irradiance conditions after 10 min preconditioning; both device types show a wavelength-dependent bias light response with opposite trends.

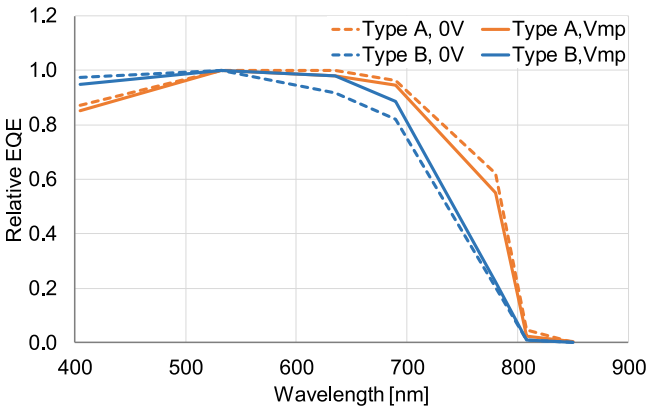


Fig. 6. Relative EQE at 0 V and V_{MPP} voltage bias at steady-state 1 Sun illumination measured after 10 min preconditioning.

From Fig. 5, it is observed that both samples show wavelength dependency on bias irradiance but with opposite trends. The effect on MMF between measuring without bias light and at 1 Sun is in this case 0.01% for type A and 0.2% for type B. Note, as detailed in the facilities section, the temperature of the DUT was not controlled during measurements. Therefore, some of the effects seen in Fig. 5 may be caused by temperature drift.

Fig. 6 illustrates the change in relative EQE influenced by voltage load after preconditioning. Both devices show significant wavelength dependence to bias voltage. However, again, the trend between both samples is different. Device A shows a reduction of NIR response with increase in voltage, while device B benefits from increased voltage up to V_{MPP} (and then drops off thereafter, not illustrated). The effect on MMF between measuring at 0 V bias and at V_{MPP} load is in this case 0.13% for type A and 0.2% for type B.

For MMF corrections of *I–V* curve measurements at standard test conditions (STC), the wavelength dependence with irradiance bias and voltage load means that the EQE should be measured using 1 Sun bias light and 0 V load to obtain a more representative MMF for I_{SC} correction. Furthermore, to correct the effects of spectral mismatch on efficiency at maximum

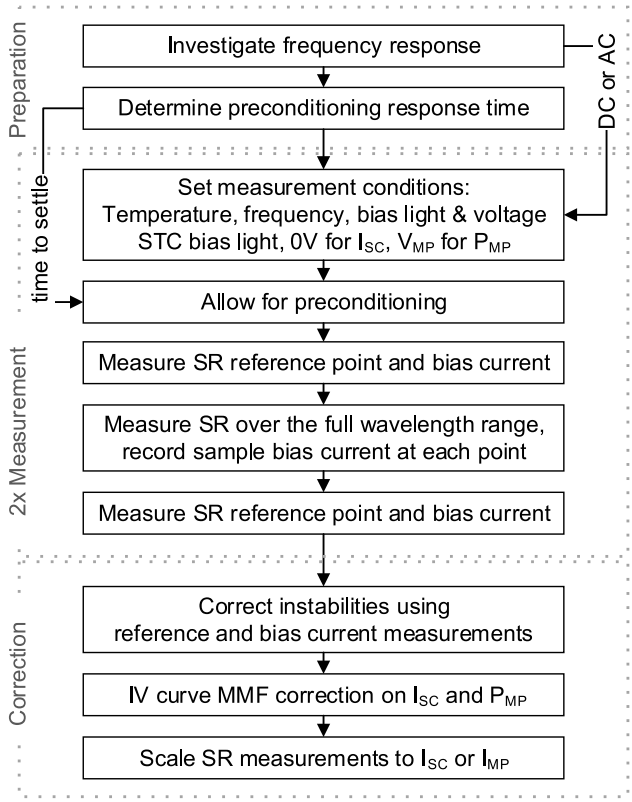


Fig. 7. Proposed universally applicable SR measurement and correction routine; the methodology presented was developed with instabilities of perovskite devices in mind.

power point, EQE should also be determined at V_{MPP} load with 1 Sun bias light intensity.

IV. Proposed Universally Applicable Measurement Routine

The results presented in the previous sections highlight the need for SR to be measured with correct measurement bias while allowing for preconditioning to not introduce additional errors in the MMF corrections. Fig. 7 proposes a universally applicable measurement routine to achieve accurate and reproducible SR measurements at low uncertainty. The flowchart can be separated into three sections: preparation, measurement, and correction.

Measurement preparation can be done on same type/batch samples if very fast device degradation is a problem. The target is to determine broadly the SR measurement frequency response and its effect on the shape of the EQE curve. If shape is not affected, one can measure using a suitable ac measurement frequency (within a flat response area). Changes in the absolute scale of the SR curve are corrected for in the subsequent correction phase and most importantly do not affect MMF. The preconditioning response time needs to be determined to estimate how long it takes for stabilization of the bias current under bias irradiance and voltage load and how stable the current signal is over the entire SR measurement. Because some devices show a slow change in performance after the initial

preconditioning, it is not advisable to wait until the effect has fully stabilized, due to the long waiting time that may also induce device degradation. Therefore, the time to precondition should be determined based on how long the actual SR measurement takes after preconditioning. As a guideline value, to achieve a good SR curve correction accuracy, the current signal should not change by more than 5% over the time in which the SR curve is measured. If the DUT shows high instability and fast degradation, the guideline value should be relaxed to what is achievable and a shorter preconditioning time should be used.

Because both test device types showed wavelength dependence on voltage load, two SR curve measurements should be carried out: one to correct for I_{SC} and one for P_{MPP}. If device degradation is a problem and prevents two measurements, P_{MPP} is probably the more important parameter to correct the device efficiency for spectral mismatch.

To correct for instability and possible degradation of the DUT during measurements, the SR reference point measurements before and after SR curve tracing should be made at a wavelength with good response from the DUT. Furthermore, the DUT's bias current should be recorded throughout measurements at every point taken in the SR curve. From this, the stability throughout the measurements can be determined and corrected for.

The third part of the methodology details the corrections applied to the SR measurements and *I–V* curve parameters. Provided that the bias light intensity and device temperature are stable, the SR reference point measurements combined with the recorded bias currents can be used to correct the SR curve for instability in performance and thus for errors in SR shape that affect MMF corrections. Changes in bias current will in the first order affect the absolute scale of the SR curve, thus the following equation can be used to correct each point in the SR curve:

$$\mathrm{SR}_C = \mathrm{SR}_M \left(1 - \frac{(C_M - C_1)(R_2 - R_1)}{(C_2 - C_1) R_1}\right) \qquad (1)$$

where R_1, R_2 and C_1, C_2 are the reference SR and DUT bias current readings, respectively, SR_M is the measured SR value and C_M the bias current at SR_M. The limitation of the stability correction is that it cannot correct for wavelength dependent instability of the DUT. However, as detailed bias current affects absolute scale in the first order, the correction proposed here will still improve the measurement result. The corrected SR curve can then be used for MMF corrections according to [12]. To correct the absolute scale of the SR curve, the MMF corrected current (I_{SC} or I_{MPP}) can be used.

The proposed methodology is to some extent simplified to allow for ease of use, to reduce measurement time, and the effects of possible degradation of devices during measurements. Ideally, to achieve the correct SR curve of a nonlinear solar cell with wavelength dependence on irradiance bias, one should measure the EQE as a function of irradiance bias [31], [32]. This is because most systems do not measure absolute SR but differential SR using an alternating low power monochromatic light beam on top of a broadband bias light. However, this would take a long time and the reduction in uncertainty would be likely secondary to other uncertainty factors, i.e., the impact on combined uncertainty would be a minor factor, especially for devices that exhibit rapid performance degradation. Taking only measurements at 1 Sun bias light intensity (one at 0 V and one at V_{MPP}) provides a very good first approximation. If lowest uncertainty is required, one should measure SR as a function of bias light and voltage load. The complete *I–V* curve can then be corrected using voltage dependent MMF.

V. Conclusion

This work has proposed a universally applicable SR measurement routine for perovskite solar cells. It was developed with R&D laboratories in mind and, as detailed, can be extended in detail when the lowest uncertainty is required by calibration laboratories. It consists of three parts (preparation, measurement, and correction) to ensure the correct measurement conditions are used and measurements are corrected for instability of the sample performance. The measurement method was developed based on the investigation of the influence of frequency, preconditioning, light intensity, and voltage load on the SR of two different types of perovskite device. It has been observed that while both architectures show significant influences in all factors, this is often with opposite trends, which makes universal prediction of the response of different perovskite solar cells difficult. This has highlighted the need to verify the response of new devices to ensure measurement accuracy, which is an integral part of the presented measurement method. This preliminary characterizing stage makes the method applicable not only to the device types tested, but for all devices. The most important characteristic observed was that both device types show wavelength dependent response with incident light intensity and applied voltage. This means that SR should at least be measured at short circuit and maximum power points at STC to correct both points for spectral mismatch.

Overall, this newly proposed method with the recommendations given lowers uncertainty in SR measurements and therefore also increases accuracy in *I–V* curve MMF corrections. This will improve comparability of sample performance and measurements between laboratories. The benefit is not limited to calibration laboratories but includes academic and R&D laboratories taking the first measurements, as it can help them to clearly identify and compare good cells and to be able to acknowledge actual performance improvements due to materials and/or processing, i.e., only when such improvements are larger than measurement uncertainty and repeatability.

References

[1] M. A. Green *et al.*, "Solar cell efficiency tables (version 51)," *Progr. Photovolt. Res. Appl.*, vol. 26, no. 1, pp. 3–12, Jan. 2018, doi: 10.1002/pip.2978.

[2] W. S. Yang *et al.*, "High-performance photovoltaic perovskite layers fabricated through intramolecular exchange," *Science*, vol. 348, no. 6240, pp. 1234–1237, Jun. 2015, doi: 10.1126/science.aaa9272.

[3] P. Calado *et al.*, "Evidence for ion migration in hybrid perovskite solar cells with minimal hysteresis," *Nature Commun.*, vol. 7, 2016, Art. no. 13831, doi: 10.1038/ncomms13831.

[4] O. Almora, C. Aranda, I. Zarazua, A. Guerrero, and G. Garcia-Belmonte, "Noncapacitive hysteresis in perovskite solar cells at room temperature," *ACS Energy Lett.*, vol. 1, no. 1, pp. 209–215, 2016, doi: 10.1021/acsenergylett.6b00116.

[5] H. J. Snaith *et al.*, "Anomalous hysteresis in perovskite solar cells," *J. Phys. Chem. Lett.*, vol. 5, no. 9, pp. 1511–1515, 2014, doi: 10.1021/jz500113x.
[6] W. Tress *et al.*, "Understanding the rate-dependent J–V hysteresis, slow time component, and aging in $CH_3NH_3PbI_3$ perovskite solar cells: The role of a compensated electric field," *Energy Environ. Sci.*, vol. 8, no. 3, pp. 995–1004, 2015, doi: 10.1039/C4EE03664F.
[7] G. Garcia-Belmonte and J. Bisquert, "Distinction between capacitive and noncapacitive hysteretic currents in operation and degradation of perovskite solar cells," *ACS Energy Lett.*, vol. 1, no. 4, pp. 683–688, Oct. 2016, doi: 10.1021/acsenergylett.6b00293.
[8] R. B. Dunbar *et al.*, "How reliable are efficiency measurements of perovskite solar cells? The first inter-comparison, between two accredited and eight non-accredited laboratories," *J. Mater. Chem. A*, vol. 5, no. 43, pp. 22542–22558, 2017, doi: 10.1039/C7TA05609E.
[9] Y. Hishikawa, H. Shimura, T. Ueda, A. Sasaki, and Y. Ishii, "Precise performance characterization of perovskite solar cells," *Curr. Appl. Phys.*, vol. 16, no. 8, pp. 898–904, 2016, doi: 10.1016/j.cap.2016.05.002.
[10] J. A. Christians, J. S. Manser, and P. V. Kamat, "Best practices in perovskite solar cell efficiency measurements. Avoiding the error of making bad cells look good," *J. Phys. Chem. Lett.*, vol. 6, no. 5, pp. 852–857, Mar. 2015, doi: 10.1021/acs.jpclett.5b00289.
[11] E. Zimmermann *et al.*, "Characterization of perovskite solar cells: Towards a reliable measurement protocol," *APL Mater.*, vol. 4, no. 9, Sep. 2016, Art. no. 091901, doi: 10.1063/1.4960759.
[12] *Photovoltaic Devices — Part 7: Computation of the Spectral Mismatch Correction for Measurements of Photovoltaic Devices*, IEC 60904-7, 2008.
[13] *Photovoltaic Devices - Part 3: Measurement Principles for Terrestrial Photovoltaic (PV) Solar Devices With Reference Spectral Irradiance Data*, IEC 60904-3, 2016.
[14] O. Dupré, R. Vaillon, and M. A. Green, *Thermal Behavior of Photovoltaic Devices*. Cham, Switzerland: Springer, 2017, doi: 10.1007/978-3-319-49457-9.
[15] W. L. Leong *et al.*, "Identifying fundamental limitations in halide perovskite solar cells," *Adv. Mater.*, vol. 28, no. 12, pp. 2439–2445, Mar. 2016, doi: 10.1002/adma.201505480.
[16] W. Chen *et al.*, "Efficient and stable large-area perovskite solar cells with inorganic charge extraction layers," *Science.*, vol. 350, no. 6263, pp. 944–948, Nov. 2015, doi: 10.1126/science.aad1015.
[17] M. Saliba *et al.*, "Cesium-containing triple cation perovskite solar cells: Improved stability, reproducibility and high efficiency," *Energy Environ. Sci.*, vol. 9, no. 6, pp. 1989–1997, 2016, doi: 10.1039/C5EE03874J.
[18] J. Baker *et al.*, "High throughput fabrication of mesoporous carbon perovskite solar cells," *J. Mater. Chem. A*, vol. 5, no. 35, pp. 18643–18650, 2017, doi: 10.1039/C7TA05674E.
[19] G. Grancini *et al.*, "One-year stable perovskite solar cells by 2D/3D interface engineering," *Nature Commun.*, vol. 8, no. 14, Jun. 2017, Art. no. 15684, doi: 10.1038/ncomms15684.
[20] *Photovoltaic (PV) Module Performance Testing and Energy Rating - Part 9: Solar Simulator Performance Requirements*, IEC 60904-9, p. 16, 2007.
[21] D. L. Young, B. Egaas, S. Pinegar, and P. Stradins, "A new real-time quantum efficiency measurement system," in *Proc. 33rd IEEE Photovolt. Spec. Conf.*, 2008, vol. 80401, pp. 1–3, doi: 10.1109/PVSC.2008.4922748.
[22] G. Bardizza, D. Pavanello, H. Müllejans, and T. Sample, "Spectral responsivity measurements of DSSC devices at low chopping frequency (1 Hz)," *Progr. Photovolt. Res. Appl.*, vol. 24, no. 4, pp. 428–435, Apr. 2016, doi: 10.1002/pip.2558.
[23] J. Hohl-Ebinger, A. Hinsch, R. Sastrawan, W. Warta, and U. Wurfel, "Dependence of spectral response of dye solar cells on bias illumination," in *Proc. 19th Eur. Photovolt. Solar Energy Conf.*, 2004, pp. 173–175.
[24] X.-Z. Guo *et al.*, "Study on the effect of measuring methods on incident photon-to-electron conversion efficiency of dye-sensitized solar cells by home-made setup," *Rev. Sci. Instrum.*, vol. 81, no. 10, Oct. 2010, Art. no. 103106, doi: 10.1063/1.3488456.
[25] Y. Hishikawa, M. Yanagida, and N. Koide, "Performance characterization of the dye-sensitized solar cells," in *Proc. Conf. Rec. 31st IEEE Photovolt. Spec. Conf.*, 2005, pp. 67–70, doi: 10.1109/PVSC.2005.1488070.
[26] X. Yang, M. Yanagida, and L. Han, "Reliable evaluation of dye-sensitized solar cells," *Energy Environ. Sci.*, vol. 6, no. 1, pp. 54–66, 2013, doi: 10.1039/C2EE22998F.
[27] D. J. Wehenkel, K. H. Hendriks, M. M. Wienk, and R. A. J. Janssen, "The effect of bias light on the spectral responsivity of organic solar cells," *Org. Electron.*, vol. 13, no. 12, pp. 3284–3290, Dec. 2012, doi: 10.1016/j.orgel.2012.09.040.
[28] H. Müllejans and H. Bossong, "Temperature and bias light dependence of spectral response measurements," in *Proc. PV Technol. Energy Solution,* Rome, Italy, 2002, pp. 891–894.
[29] C. J. Hibberd *et al.*, "Voltage-dependent quantum efficiency measurements of amorphous silicon multi-junction mini-modules," *Sol. Energy Mater. Sol. Cells*, vol. 95, no. 1, pp. 123–126, Jan. 2011, doi: 10.1016/j.solmat.2010.03.039.
[30] C. Monokroussos *et al.*, "Effects of spectrum on the power rating of amorphous silicon photovoltaic devices," *Progr. Photovolt. Res. Appl.*, vol. 19, no. 6, pp. 640–648, Sep. 2011, doi: 10.1002/pip.1080.
[31] J. Metzdorf, "Calibration of solar cells 1: The differential spectral responsivity method," *Appl. Opt.*, vol. 26, no. 9, pp. 1701–1708, May 1987, doi: 10.1364/AO.26.001701.
[32] S. Winter *et al.*, "Design, realization and uncertainty analysis of a laser-based primary calibration facility for solar cells at PTB," *Measurement*, vol. 51, no. 1, pp. 457–463, May 2014, doi: 10.1016/j.measurement.2013.12.001.

Authors' photographs and biographies not available at the time of publication.